-92-12A

COBE-PREPRINT-NO-92-12A

Fermilab Library
0 1160 0020176 8

COBE/DIRBE OBSERVATIONS OF INFRARED EMISSION FROM STARS AND DUST

Michael G. Hauser
Code 680, NASA Goddard Space Flight Center, Greenbelt, MD 20771.

ABSTRACT

The Diffuse Infrared Background Experiment (DIRBE) on NASA's Cosmic Background Explorer (*COBE*) satellite has obtained low- angular resolution photometric maps of the full sky in ten broad spectral bands from 1.2 to 240 μm wavelength, and linear polarization maps at 1.2, 2.3, and 3.5 μm. These maps provide dramatic new views of the interplanetary dust cloud, integrated stellar light, and dust in the interstellar medium. An empirical function is used to separate the contribution from interplanetary dust, facilitating study of the stellar and interstellar emissions from the plane of the Milky Way. Initial results of such studies are presented in accompanying papers.

1. INTRODUCTION

The primary aim of the Diffuse Infrared Background Experiment is to conduct a definitive search for the isotropic cosmic infrared background radiation. This objective, and preliminary results of that search, have been discussed by Hauser et al. (1991). Additional objectives of the DIRBE are study of the diffuse interplanetary and interstellar media. To accomplish these objectives, the DIRBE was designed to obtain absolute brightness maps of the full sky in ten broad photometric bands from 1.2 to 240 μm wavelength. To facilitate study of the bright foreground contribution from interplanetary dust, linear polarization was also measured at 1.2, 2.2, and 3.5 μm, and all celestial directions were observed hundreds of times at all accessible elongation angles from the Sun in the range 64° to 124°.

A careful photometric reduction of the data from this unprecedentedly extensive infrared sky survey is currently in progress. In this paper, full sky images prepared from DIRBE data obtained during the initial five months of the *COBE* mission are presented. An empirical approach useful for separating the sky brightness contribution from interplanetary dust scattering and emission is described. Residual errors from this separation are small at low galactic latitude, facilitating studies of large scale galactic properties appropriate to the aims of this Conference. The specific investigations undertaken are described in accompanying papers at this Conference: stellar colors and extinction (Arendt *et al.* 1993); structure of the stellar bulge and implications for a stellar bar in the Milky Way (Weiland *et al.* 1993); large scale conditions in the interstellar medium (Sodroski *et al.* 1993); evidence for the galactic warp in the stellar and interstellar galactic components (Freudenreich *et al.* 1993); and a preliminary report on polarimetry with the DIRBE data (Berriman *et al.* 1993). The reader is referred to the above papers for the results of these DIRBE investigations. Implications of data from the *COBE* Far Infrared Absolute Spectrophotometer for the cooling of the interstellar gas are presented at this Conference by Bennett & Hinshaw (1993), and for the presence of very cold interstellar dust by Wright

C 92/10/12.1

(1993).

2. THE *COBE* MISSION AND DIRBE INSTRUMENT

The DIRBE was one of three instruments launched aboard the *COBE* satellite on Nov. 18, 1989. The *COBE* was placed in a circular, 900-km altitude, Sun-synchronous terminator orbit. The DIRBE was located inside a superfluid helium dewar which provided operating temperatures from 1.5 to 3 K for the various parts of the instrument from launch until expiration of the helium on Sept. 21, 1990. Since helium expiration, the interior of the dewar has stabilized near 50 K, cold enough for continued operation of the DIRBE from 1.2 to 4.9 μm; such operations are planned to continue until November 1993. In this orbit, the satellite is in full sunlight continuously except for parts of each orbit during a few month interval around the June solstice. During this 'eclipse' season, thermal conditions on the spacecraft are less stable than during the rest of the year. Data presented in this paper and the accompanying studies were obtained in the interval from Dec. 12, 1989, when instrument operation was optimized for standard orbital conditions, until May 1990, when the first 'eclipse season' began. A more detailed description of the *COBE* mission and its instruments has recently been given by Boggess *et al.* (1992).

The DIRBE instrument consists of a folded, off-axis Gregorian telescope with a 19-cm diameter primary mirror and a 10-spectral band absolute photometer and 3-band polarimeter. Sky brightness is measured at wavelengths of 1.2, 2.2, 3.5, 4.9, 12, 25, 60, 100, 140, and 240 μm, and linear polarization is measured at the three shortest wavelengths. The instrument rms sensitivity per field of view in 10 months is $\lambda I(\lambda) = (1.0,\ 0.9,\ 0.6,\ 0.5,\ 0.3,\ 0.4,\ 0.4,\ 0.1,\ 11.0,\ 4.0) \times 10^{-9}$ W m^{-2} sr^{-1}, respectively for the ten wavelength bands listed above. These levels are generally well below the total infrared sky brightness. The optical configuration (Magner 1987) has strong rejection of stray light from the Sun, Earth limb, Moon or other off-axis celestial radiation, or parts of the *COBE* payload (Evans, 1983; Evans and Breault 1983).

The DIRBE instrument measures absolute brightness by chopping between the sky signal and a zero flux internal reference using a tuning fork chopper. Instrumental offsets are measured by closing a cold shutter located at the prime focus. All spectral bands view the same instantaneous 0.7° x 0.7° field-of-view oriented at 30° from the spacecraft spin axis, which was maintained normally at 94° from the Sun and away from the Earth. This provides modulation of the solar elongation angle by 60° during each rotation, and mapping of 50% of the celestial sphere each day. As the orbit precesses 1° each day, the DIRBE slowly increases its sky coverage until the full sky is mapped each six months. The spiral scan yields hundreds of observations of each celestial direction every half year, with elongation angle varying over the full interval accessible at its ecliptic latitude in the range 64 to 124 degrees.

Four highly-reproducible internal radiative reference sources are used to stimulate all detectors when the shutter is closed to monitor the stability and linearity of the instrument response. Calibration of the photometric scale is obtained from observations of isolated bright celestial sources. The highly redundant sky sampling and frequent response checks will allow maintenance of precise photometric closure over the sky for the duration of the mission. The data obtained during the helium temperature phase of the mission are of excellent photometric quality, showing good sensitivity, stability, linearity, and stray

light immunity. The measured sky brightnesses used for the studies presented at this Conference are conservatively estimated to have absolute photometric scale accuracy at each wavelength of 20%. Because a common celestial calibrator (Sirius) has been used from 1.2 to 12 μm, it is estimated that the accuracy of intensity ratios (colors) formed from these bands is of order 5%. Similarly, the 60 μm to 100 μm intensity ratio (common calibrator is Uranus) and 140 μm to 240 μm intensity ratio (common calibrator is Jupiter) are comparably accurate. The photometric consistency over the sky at each individual wavelength is better than 2%, except at 60 μm and 100 μm where non-linear detector effects have not yet been corrected.

3. THE APPEARANCE OF THE INFRARED SKY

Qualitatively, the initial DIRBE sky maps show the expected character of the infrared sky. This is shown in Figs. 1-4 (Color Plate numbers 3 and 4), each of which is a 3-band false color image of the full sky. Each image is a Mollweide projection in galactic coordinates, with the galactic center at the center of the image. In each case, the intensity at each wavelength is represented by the blue, green, or red intensity for the shortest to longest wavelength respectively. These images differ from earlier versions of the DIRBE data in two important respects: the data have been processed with the DIRBE pipeline software rather than 'quick-look' software, so that numerous segments of inferior data or processing artifacts have been eliminated and the full sky is included. Furthermore, the brightness shown at each sky pixel is the brightness observed when the solar elongation angle was 90°, so that there are no discontinuities in the images due to discreetly different elongations for adjacent sky pixels. This is the largest elongation angle for which the whole sky can be observed. The DIRBE, because of its dense sampling of each sky pixel at all possible elongation angles in the range 64° to 94°, has provided the first data set for which such images can be made.

Figure 1 shows a composite of the 1.2, 2.2, and 3.5 μm images. At 1.2 μm, stellar emission from the galactic plane and from isolated high latitude stars is prominent. Zodiacal scattered light from interplanetary dust is also present, but is so much fainter than starlight from the galactic disk that it is not apparent within the dynamic range displayed in Fig. 1. These two components continue to dominate out to 3.5 μm, though both become fainter as wavelength increases. Because extinction at these wavelengths is far less than in visible light, the disk and bulge stellar populations of the Milky Way are dramatically apparent in this image. Since extinction decreases from 1.2 to 3.5 μm wavelength, the image appears redder where there is more extinction, *e.g.*, in the plane of the disk and in discrete clouds in the northern part of the bulge.

Figure 2 shows a composite of the 4.9, 12, and 25 μm images. At 12 and 25 μm, emission from the interplanetary dust dominates the sky brightness everywhere but the central part of the galactic disk. This is evident in the bright S-shaped band, which is centered on the ecliptic plane. As with the scattered zodiacal light, the emitted contribution from the interplanetary dust decreases with increasing ecliptic latitude and with increasing solar elongation angle. The hard edges on the interplanetary dust emission on either side of the ecliptic plane are the result of emission from the zodiacal dust bands, first noted in the *IRAS* data by Low *et al.* (1984). Scattered light from these bands has also been detected at near-infrared wavelengths in the DIRBE data (Weiland *et al.* 1991).

Figure 3 shows a composite of the 25, 60, and 100 μm images. At wave-

lengths of 60 μm and longer, emission from the interstellar medium dominates the galactic brightness, and the interplanetary dust emission becomes progressively less intense and hence appears blue in this image. The patchy infrared cirrus noted in IRAS data (Low *et al.* 1984) is evident at all wavelengths longer than 25 μm. Numerous nearby molecular clouds are evident in the image, such as the ρ Oph cloud North of the galactic center and the Orion complex below the plane at the right. Both Magellanic Clouds are also evident.

Figure 4 shows a composite of the 100, 140, and 240 μm images. The interplanetary dust and stellar contributions have nearly vanished, leaving a nearly uniform-temperature interstellar medium dominating the image. The series of images in Figs. 1-4 show clearly the changing character of the sky as source temperatures progress from thousands of degrees to tens of degrees. The DIRBE data will clearly be a valuable new resource for studies of the interplanetary medium and Galaxy as well as the search for the cosmic infrared background radiation.

4. REMOVAL OF THE INTERPLANETARY DUST SIGNAL

In order to carry out the quantitative studies of large- scale galactic properties described in the accompanying papers, an empirical procedure has been used to remove much of the foreground signal from the interplanetary dust (IPD). The procedure entails fitting an analytic function approximating the expected large- angular scale features of the IPD to the maps constructed from data at elongation angle 90°. Properties of the IPD cloud considered in choosing this function include the facts that the cloud is approximately an azimuthally symmetric distribution centered near the Sun and concentrated toward a symmetry surface, that this surface is inclined by a small angle with respect to the ecliptic plane, and that the dust density falls off rather rapidly with increasing distance from the Sun. This suggests that at high ecliptic latitude, β, the distribution should be close to a $\csc(\beta)$ distribution, which rounds off to a finite value as the symmetry surface is approached, and that the latitude of maximum brightness is not in general zero (though it is at that time of year when the Earth is in the line of nodes of the symmetry surface with the ecliptic plane). This suggests an expression for the intensity I at fixed elongation angle of the form:

$$I = I_o - k\{1 - \beta_c|\csc(\beta - \beta_o)|[1 - \exp(-x - \alpha x^2)]\}$$

where I_o = peak intensity, β_o = ecliptic latitude at maximum intensity, β_c = width parameter of the IPD brightness profile, k = intensity scale factor which defines the plane to pole intensity contrast, and $x = |(\beta - \beta_o)/\beta_c|$.

The parameter α can be chosen to minimize residuals. Though the value $\alpha = 1/2$ gives a profile with zero slope at $\beta = \beta_o$, one finds systematically smaller residuals for α values near 1/3. With the choice of $\alpha = 1/3$, the maximum residuals are typically a few percent of the peak IPD brightness and are dominated by the zodiacal band structure discovered in the *IRAS* data (Low *et al.* 1984).

This empirical function has been fitted separately to 1/4 -great circle map data segments at fixed ecliptic longitude from each ecliptic pole to the ecliptic latitude of maximum IPD intensity, β_o (recall that the solar elongation angle is fixed at 90° in these maps). The values of I_o and β_o in the ecliptic northern and southern segments of each 1/2 -great-circle at the same ecliptic longitude were required to be the same. This results in six free parameters for each half

great-circle, and yields low residuals, particularly for the low galactic latitude regions studied here. Estimated residual contamination of the resulting 'galactic emission' maps by IPD signal depends on wavelength, and is noted in the accompanying papers. It might be noted that any constant contribution to the sky brightness (or instrument signal) over these data segments is included in the constant I_o, and does not appear in the residual 'galactic' emission maps.

5. CONCLUSIONS

The DIRBE instrument has provided extensive new data with many unique attributes showing the character of diffuse celestial emission from 1.2 to 240 μm wavelength. In particular, these data reveal large-scale properties of both the stellar and interstellar components of the Galaxy. A simple empirical fitting function permits removal of foreground solar system sky brightness contributions with small systematic residuals compared to galactic signals near the galactic plane. Some implications for the galactic bulge and disk are presented in five companion papers at this Conference.

ACKNOWLEDGEMENTS

The author gratefully acknowledges the contributions of his colleagues on the *COBE* Science Working Group to the accomplishments described here. He acknowledges particularly the contributions of N. Boggess, T. Kelsall, S. H. Moseley, R. F. Silverberg, and J. Weiland to this paper. The staff of the Cosmology Data Analysis Center, and particularly the *COBE* pipeline software development teams led by J. A. Skard and G. Toller, are thanked for their tireless efforts in producing the careful reduction of the data used in this investigation.

COBE is supported by NASA's Astrophysics Division. Goddard Space Flight Center (GSFC), under the scientific guidance of the *COBE* Science Working Group, is responsible for the development and operation of *COBE*.

REFERENCES
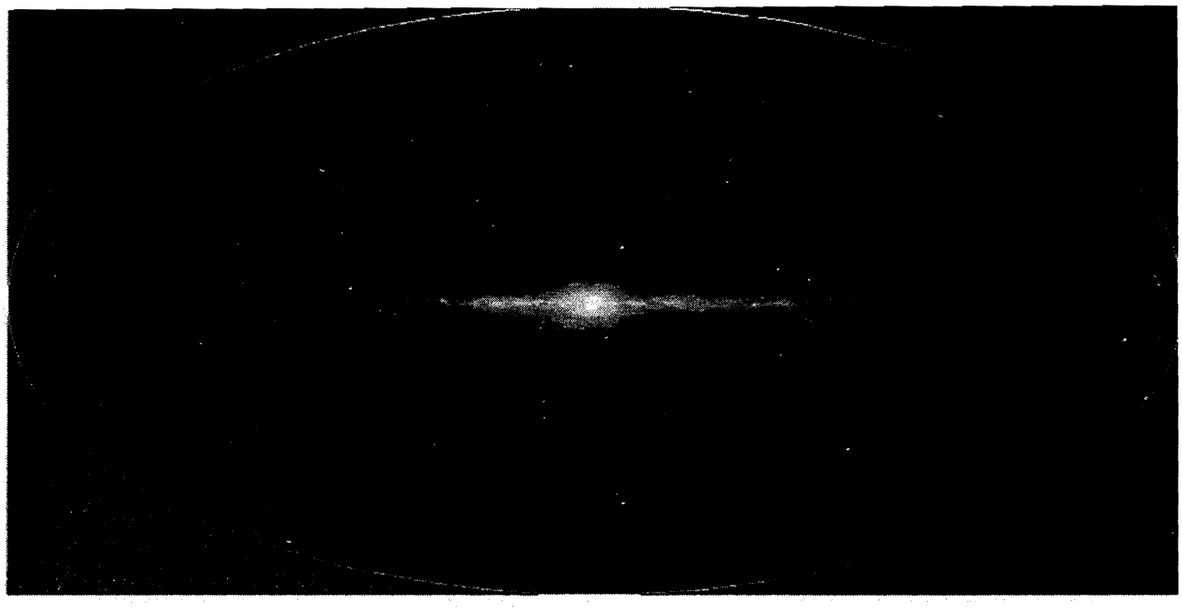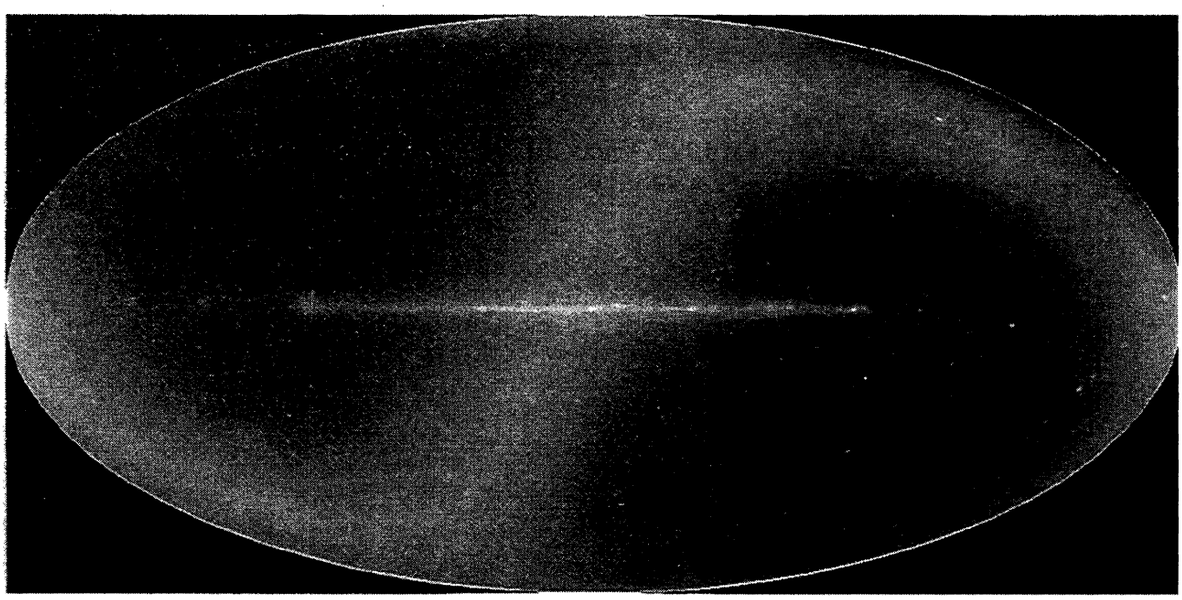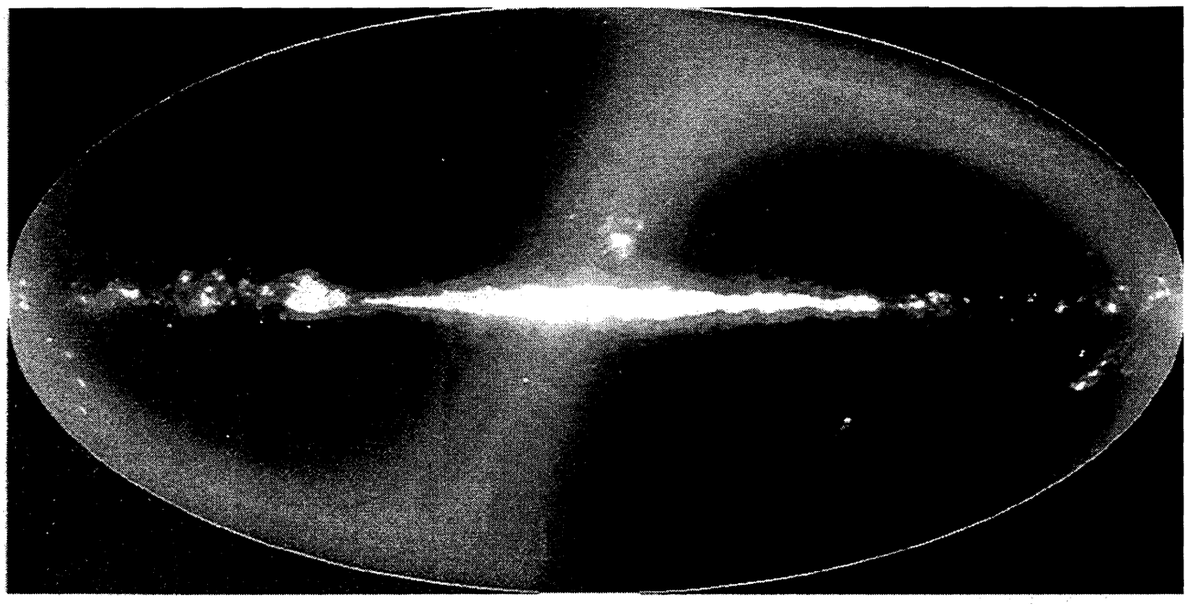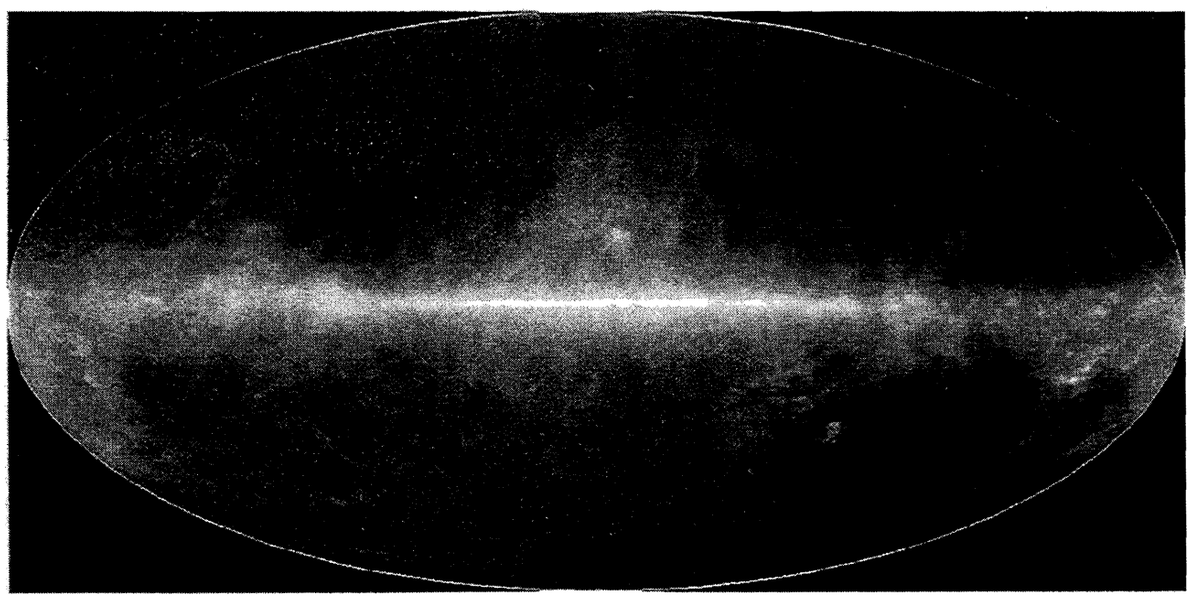
Arendt, R. G. *et al.* 1993, this volume
Bennett, C. L. & Hinshaw, G. 1993, this volume
Berriman, G. B. *et al.* 1993, this volume
Boggess, N. *et al.* 1992, ApJ, 397, 420
Evans, D. C. 1983, SPIE Proc., 384, 82
Evans, D. C.& Breault, R. P. 1983, SPIE Proc., 384, 90
Freudenreich, H. T. *et al.* 1993, this volume
Hauser, M. G. *et al.* 1991, in "After the First Three Minutes", eds. S. S. Holt, C. L. Bennett, V. Trimble, (AIP: New York), p. 161
Low, F. J. *et al.* 1984, ApJ, 278, L19
Magner, T. J. 1987, Opt. Eng., 26, 264
Sodroski, T. J. *et al.* 1993, this volume
Weiland, J. L. *et al.* 1991, BAAS, 23, 1313
Weiland, J. L. *et al.* 1993, this volume
Wright, Edward L. 1993, this volume